ISBN: 978-3-95450-168-7 doi:10.18429/JACoW-IPAC2015-MOPMA003

RECONSTRUCTION OF ELECTRON BUNCH MOTION DURING CSR BURSTS USING SYNCHRONISED DIAGNOSTICS

I.P.S. Martin, C. Bloomer, L.M. Bobb, A. Finn, G. Rehm, Diamond Light Source, Oxfordshire, U.K.
R. Bartolini, Diamond Light Source, Oxfordshire, U.K.
John Adams Institute, University of Oxford, U.K.

Abstract

Above a certain threshold current, electron bunches become unstable and emit bursts of coherent synchrotron radiation (CSR). The character and periodicity of these bursts vary with bunch current, RF voltage and lattice momentum compaction. In this paper we describe recent measurements taken at Diamond of how the electron bunch longitudinal profile and energy vary during a burst, and correlate this with CSR emission at a range of wavelengths.

INTRODUCTION

The onset of microbunching instabilities in storage rings is a well known phenomenon [1, 2]. These occur when the current stored in an electron bunch exceeds a certain threshold value, at which point the interaction of the bunch with its own wakefields is sufficiently strong to cause density modulations to occur within the bunch. These in turn increase the amplitude of the wakefields, giving rise to an instability. For a given storage ring, the current threshold is found to vary both with RF voltage and momentum compaction.

In recent years the subject of CSR-driven microbunching has received considerable attention due to its detrimental effects both in rings and in linac bunch compressors [3–9]. In the case of rings, this attention has been mainly focussed on rings with positive momentum compaction, with little experimental evidence for negative momentum compaction lattices. Such data would provide a useful benchmark against which numerical simulations could be compared [10], as well be valuable for its wider academic interest. It is also of particular relevance for Diamond Light Source, as the ring is regularly operated in a negative low-alpha configuration for the generation of both coherent THz radiation and short x-ray pulses [11].

In this paper we describe recent measurements taken at Diamond Light Source in low-alpha mode that characterise the electron bunch motion during CSR bursts. These are correlated with mm-wave emissions recorded using a selection of Schottky Barrier Diodes, thus giving further insight into the underlying electron beam dynamics.

CSR BURST DETECTION

The microbunching instability primarily affects the longitudinal phase space of the electron bunch. As such, the most important observables to measure are the electron bunch length, bunch arrival time and bunch energy. Ideally one would also like to measure the internal bunch structure and energy spread during a burst; however, this is not yet possible using the diagnostics available at Diamond.

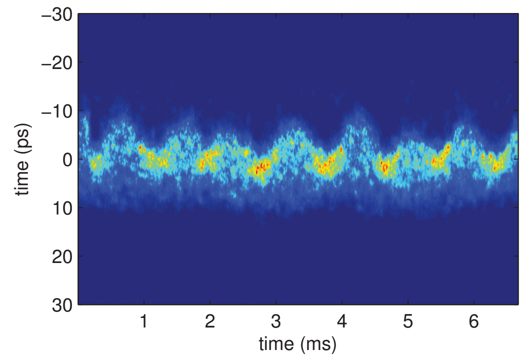

Figure 1: Streak camera image capturing CSR bursts for $\alpha_1 = -4.6 \times 10^{-6}$, $V_{RF} = 3.4$ MV, $I_{bunch} = 39.5\mu$A.

The electron bunch length and arrival time is recorded using an Optronis dual-sweep streak camera [12]. In recent years, the performance of this camera at Diamond has been optimised by the introduction of a fully reflective front-end optics and pinhole located upstream of the camera, alongside a post-processing of the recorded images by deconvolving them with the measured point-spread function [13]. An example of one such measurement is shown in Fig. 1.

The electron bunch energy is measured indirectly using the turn-by-turn BPM system. During a burst the electron bunch loses energy to the radiation field, causing it to undergo coherent synchrotron oscillations. This energy deviation can be measured from the transverse offset at positions of high dispersion, assuming the dispersion amplitude is known. The picture is slightly complicated by the presence of additional betatron oscillations. However, by averaging across BPMs of similar dispersion, and by filtering out the high-frequency betatron contributions, the mean energy deviation of the bunch can be recovered.

Whilst it is not possible to directly observe the internal structure of the electron bunches at Diamond, the detection of the accompanying CSR bursts using Schottky Barrier Diodes (SBDs) serves as a useful proxy. The detectors used during these measurements have sensitivity bandwidths of 33-50 GHz, 60-90 GHz, 90-140 GHz, 140-220 GHz, 220-330 GHz, 330-500 GHz and 500-750 GHz. These frequencies correspond to periods in the range 1.3-30 ps, and the detectors at the higher frequency end of the range in particular should be sensitive to sub-structure appearing within the electron bunch. The SBD array used during these studies is described in more detail in a companion paper [14].

ISBN: 978-3-95450-168-7 doi:10.18429/JACoW-IPAC2015-MOPMA003

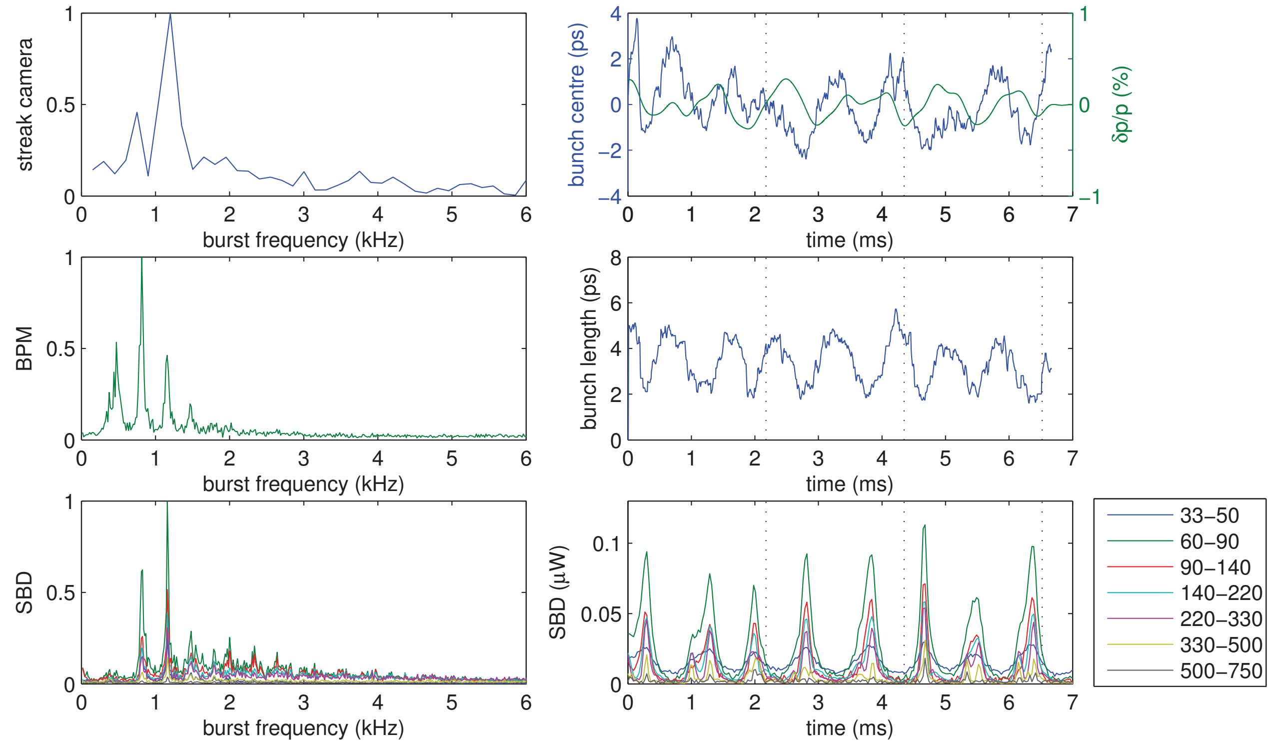

Figure 2: Overview of measurements for $\alpha_1 = -4.6 \times 10^{-6}$, $V_{RF} = 3.4$ MV, $I_{bunch} = 39.5\mu$A. Top left: FFT of the bunch length data. Middle left: FFT of the beam energy as a function of time extracted from the high-dispersion BPMs. Bottom left: FFT of the SBD data. Top right: Bunch arrival time and beam energy measured by the streak camera and EBPMs respectively. Middle right: Bunch length extracted from the streak camera data. Bottom Right: SBD data. The dashed vertical lines on the right-hand figures indicate the synchrotron period ($f_s = 460$ Hz).

MEASUREMENT RESULTS

Measurements of the electron bunch motion have been acquired for a range of values of α_1 and for increasing I_{bunch}. All measurements were taken in single bunch mode, with the RF cavity voltage set to 3.4 MV. This data was then processed to extract bunch length, arrival time and mean energy, as well as to determine the threshold current for the onset of instabilities. The SBDs were used to determine the power radiated in different bandwidths as a functions of α_1 and I_{bunch}. The synchronisation of the various detectors was confirmed by using the vertical 'pinger' magnet to kick the beam out on a single turn, with the data acquired in this way also serving as a good measure of the temporal resolution of each of the three detector types. An overview of the data acquired in one such measurement is shown in Fig. 2, recorded when the bunch current is just above threshold.

Time Domain

For the data shown in Fig. 2, the first point to note is that there is good correlation between the CSR amplitude measured across all SBDs and the reduction in bunch length as measured by the streak camera. This is particularly true of the long wavelength 33-50 GHz detector; however, there is some evidence of several bursts occurring on occasion on the higher frequency detectors. This suggests that some bursts occur as a result of modulation in the longitudinal bunch profile as a whole, whilst for others there is also a degree of sub-structure moving through the bunch.

The data acquired using the streak camera can also be used to examine the longitudinal bunch profile during a burst (see Fig. 3). The data indicates that, at the peak of the burst, the bunch length and energy are at a minimum and the current density is at its highest (blue line in Fig. 3). After the burst, the bunch centroid becomes delayed in time, the electrons start to gain energy, and the bunch profile elongates and leans toward the tail (green line).

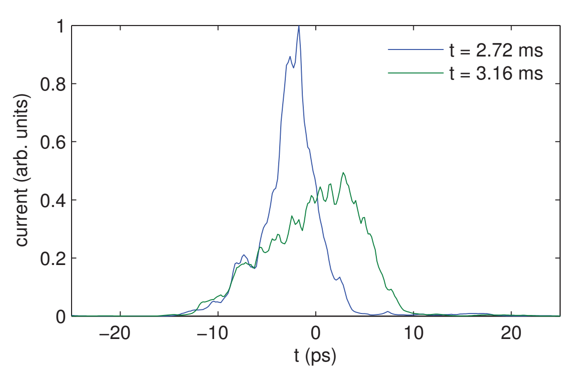

Figure 3: Bunch profile during a burst (see also Fig. 2). The head of the bunch is to the left of the figure.

ISBN: 978-3-95450-168-7 doi:10.18429/JACoW-IPAC2015-MOPMA003

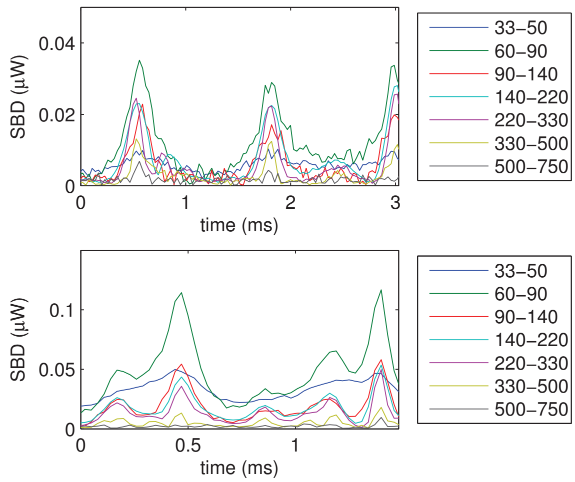

Figure 4: SBD data for α_1=-2.4×10^{-6} / I_{bunch}=21.0 μA (top) and α_1=-9.9×10^{-6} / I_{bunch}=63.9μA (bottom). In each case, data for one synchrotron period is shown.

The character of the bursts changes depending upon the length of the bunch. Shown in Fig. 4 are two cases. The first shows SBD data measured for a short electron bunch ($\alpha_1 = -2.4 \times 10^{-6}$, top) and the second is for a relatively long electron bunch ($\alpha_1 = -9.9 \times 10^{-6}$, bottom). In each case, data for a single synchrotron period is shown.

For the shorter electron bunch (σ_t = 2.7ps), the SBDs detect single bursts of radiation across all frequencies, consistent with a modulation of the longitudinal bunch profile as a whole. For the longer bunch case (σ_t = 3.6ps), there appear to be several bursts of growing amplitude seen by the shorter wavelength detectors for each burst in the 33-50 GHz detector, consistent with sub-structure within the bunch. Note that for the parallel plate model, the CSR shielding cut-off frequency at Diamond is 63.8 GHz ($\lambda_{cut-off}$ = 4.7mm). This suggests the CSR gain would peak for reduced wavelengths of $\lambda\!\!\!^{-}$ = 0.75mm (2.5 ps), similar to the measured bunch length for the $\alpha_1 = -2.4 \times 10^{-6}$ case [4].

Frequency Domain

By taking the Fourier transform of the time series from each detector, the frequency at which each signal is modulated can be found. In general, all the measurements show a similar pattern. At low currents, the bunch is stable and no modulation in bunch length, energy deviation or SBD signal can be seen. The first sign of an instability appears as a broad feature spanning several kHz in the SBD spectrum, with several sharper peaks superimposed on top of this. As the bunch current passes above the bursting threshold, the amplitude of the signal detected by the SBDs increases sharply, and more lines appear in the spectrum roughly centred at harmonics of the synchrotron frequency (n = 2 or higher). At this point, modulation of the streak camera and BPM data is also visible in their respective spectra.

A specific example above the bursting threshold is shown in the left-hand plots in Fig. 2. Here, the energy deviation extracted from the BPM data appears to be most strongly modulated at 815 Hz (roughly 2×f_s), with significant peaks also visible at 470 Hz and 1.2 kHz. Due to the limited length of time the streak camera data was acquired for, the spectrum in this case has a poor frequency resolution. However, the strongest peaks appear to be centred at roughly 2 and 3 ×f_s.

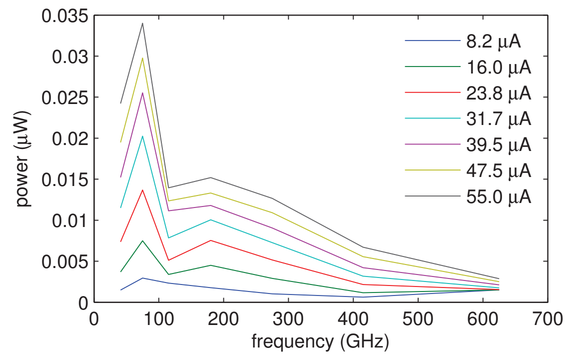

Figure 5: Measured power as a function of radiation frequency for various bunch currents ($\alpha_1 = -4.6 \times 10^{-6}$). Note that the detector noise floor increases with increasing frequency.

CSR Spectrum

Further information about the electron bunch dynamics can be inferred from the relative strength of the signal from the different SBD detectors. Assuming an approximately Gaussian bunch profile, the expectation is that above the shielding cut-off, the CSR gain (and hence measured power) will become smaller at shorter wavelengths. However, if there is a density modulation of a well defined period within the bunch, the CSR gain will also be high at this wavelength.

Across all the data sets measured with negative momentum compaction, the strongest signal was recorded using the 60-90 GHz detector. An example of this is shown in Fig. 5 for the data measured for $\alpha_1 = -4.6 \times 10^{-6}$. The power measured by each detector falls away above the 60-90 GHz band, with a significant dip also apparent in the 90-140 GHz band. Whether the reduced power measured by the 33-50 GHz and 90-140 GHz detectors is due to a genuine reduction in the CSR extracted from the beam port at these frequencies, or whether it it because of unfavourable positioning of the detectors in the array or because of an error in the calibration factor for these particular sensors remains to be determined.

CONCLUSIONS

A series of data sets have been recorded in order to characterise the electron bunch motion during CSR bursts in low alpha mode at the Diamond storage ring. These measurements were carried out for a variety of bunch currents and for different values of the momentum compaction factor, and highlight the complexity of the internal bunch motion the electrons undergo during a burst. The intention is to use this data as a benchmark for future simulations.

ISBN: 978-3-95450-168-7 doi:10.18429/JACoW-IPAC2015-MOPMA003

REFERENCES

[1] G.L. Carr et al., "Observation of Coherent Synchrotron Radiation from the NSLS VUV Ring", Nucl. Inst. Meth. A **463**, 387,(2001).

[2] J.M. Byrd et al., "Observation of Broadband Self-Amplified Spontaneous Coherent Terahertz Synchrotron Radiation in a Storage Ring", Phys. Rev. Lett. **89**, 224801, (2002).

[3] G. Stupakov, S. Heifets, "Beam Instability and Microbunching due to Coherent Synchrotron Radiation", Phys. Rev. ST Accel. Beams **5**, 054402, (2002).

[4] M. Venturini, R. Warnock, "Bursts of Coherent Synchrotron Radiation in Electron Storage Rings: A Dynamical Model", Phys. Rev. Lett. **89**, 224802, (2002).

[5] K.L.F. Bane, Y. Cai, G. Stupakov, "Threshold Studies of the Microwave Instability in Electron Storage Rings", Phys. Rev. ST Accel. Beams **13**, 104402, (2010).

[6] C. Evain et al., "Spatio-temporal dynamics of relativistic electron bunches during the Micro-bunching Instability in Storage Rings", Euro Phys. Lett. **98**, 40006, (2012).

[7] E. Roussel et al., "Microbunching Instability in Relativistic Electron Bunches: Direct Observations of the Microstructures Using Ultrafast YBCO Detectors", Phys. Rev. Lett. **113**, 094801, (2014).

[8] M. Borland, "Simple Method for Particle Tracking with Coherent Synchrotron Radiation", Phys. Rev. ST Accel. Beams **4**, 070701, (2001).

[9] Z. Huang et al., "Suppression of Microbunching Instability in the Linac Coherent Light Source", Phys. Rev. ST Accel. Beams **7**, 074401, (2004).

[10] M. Atay, R. Fielder, I.P.S. Martin, R. Bartolini, "Comparison of Measurements and Simulations for Single Bunch Instability at Diamond", in Proc. IPAC 2015, Richmond, MOPMA001, (2015).

[11] I.P.S. Martin, G. Cinque, G. Rehm, C.A. Thomas, R. Bartolini, "Operating the Diamond Light Source in Low Alpha Mode for Users", in Proc. IPAC 2013, Shanghai, MOPEA070, (2013).

[12] `http://www.optronis.com/`

[13] C.A. Thomas, I.P.S. Martin, G. Rehm, "Diagnostics Beamline Optimisation and Image Processing for Sub-ps Streak Camera Bunch Length Measurement", in Proc. IBIC 2012, Tsukuba, TUPA42, (2012).

[14] A. Finn, P. Karataev, G. Rehm, "A Multi-band Single Shot Spectrometer for Observation of mm-wave Bursts at Diamond Light Source", in Proc. IPAC 2015, Richmond, MOPTY080, (2015).